

Supplementary Information

Vapor Switching of Luminescence Mechanism in a Re(V) Complex

Kenta Sasaki, Hitomi Yamate, Haruka Yoshino, Hiroki Miura, Yuushi Shimoda,
Kiyoshi Miyata, Ken Onda, Ryo Ohtani, Masaaki Ohba*

Kyushu University

Physical Measurement

Elemental analyses of carbon, hydrogen and nitrogen were carried out by the staff of technical support division graduate school of science in Kyushu University. UV-Vis absorption was measured by JASCO V-630. Infrared (IR) spectra were performed on a Perkin Elmer Spectrum Two FT-IR equipped with an ATR accessory in the range of 650–4000 cm^{-1} at room temperature. $^1\text{H-NMR}$ spectra were obtained with JEOL 600 MHz. Thermogravimetry analysis (TGA) was carried out on a Perkin Elmer STA6000 from 30 to 700 $^{\circ}\text{C}$ with a heating rate of 5 $^{\circ}\text{C min}^{-1}$ and under a dry nitrogen atmosphere with a flow rate of 19.8 ml min^{-1} . Adsorption isotherms were measured on BELSORP-max at 298K using circulating water tank. Emission quantum yields were measured by an absolute emission quantum yield measurement system (Hamamatsu Photonics C9920-02) composed of an integrating sphere, a multi-channel photodetector (Hamamatsu Photonics PMA-12), and 150 W CW xenon lamp as an excitation light source (excitation wavelength = 355 nm) at room temperature. PL quantum yield was calculated with the following equation:

$$\phi = \frac{\int I_{em} d\lambda}{\int (I_{ex}^{before} - I_{ex}^{after}) d\lambda}$$

I_{em} is the amount of photon from emission, I_{ex}^{before} is amount of photon from excitation light that nothing absorbed, and I_{ex}^{after} is amount of photon from excitation light that something absorbed. The accuracy of the instrument was confirmed by the measurement of the quantum yield of anthracene in ethanol ($\phi = 0.27$).¹ Time-resolved PL measurements were carried out using a streak camera (Hamamatsu C4780) coupled to a polychromator (SpectraPro-150, spectral resolution: ~ 10 nm, Acton Research Corporation). The detection system was synchronized to a nanosecond Nd:YAG laser (EKSPLA NT242, central wavelength : 1064 nm, pulse duration: 6 ns). Temperature-dependent PL measurements were performed using a liquid nitrogen cryostat (CoolSpeK UV USP-203-B). The samples were pumped by the third harmonic of the fundamental pulse from the Nd:YAG laser (355 nm). The polarization angles of the light for pumping and detection were set to the magic angle (54.7 deg) to avoid distortion of the temporal profiles from molecular orientation.²

PL lifetimes were estimated using the following fitting function (single exponential function convoluted with Gaussian as instrumental response function):

$$f(t) = \int A(t) \cdot B(t - \tau) d\tau \dots \textcircled{1}$$

$$A(t) = \frac{Amp1}{G_1} * \exp(-G_1 t), B(t) = \exp\left\{-\left(\frac{t}{pw}\right)^2\right\} \dots \textcircled{2}$$

$$f(t) = A_{const} + A_0 * (1 - \text{erf}(-2 * \sqrt{\ln(2)}/(\text{FWHM} * \sqrt{2}) * t)) + A_1 * \exp(-t/\tau_1) * (1 - \text{erf}(-2 * \sqrt{\ln(2)}/(\text{FWHM} * \sqrt{2}) * t)) \quad (t=x-t_0) \dots \textcircled{3}$$

Theoretical Calculation

Quantum chemical calculations based on the density functional theory were performed using the *Gauss View 6* program³ and *Gaussian 16* package.⁴ All calculations were performed with the SDD function for Re atom, 6-311+G(d) for H, C, N and O atoms and the GENIECP basis set. The ground-state structural optimization to a minimum was carried out for [ReN(CN)₄(cpy)]²⁻ unit with MeOH arbitrarily placed beneath cpy. The unit was modeled using crystal information file (cif).

Single-crystal X-ray diffraction

All Single-crystal X-ray diffraction data were collected on a Bruker SMART APEX II ULTRA CCD-detector Diffractometer, a rotating-anode (Bruker Turbo X-ray source) with graphite-monochromated Mo_{K α} radiation ($\lambda = 0.71073 \text{ \AA}$) was used. Computations were carried out on APEX2 crystallographic software package and OLEX2 software.⁵ A single crystal was mounted on a polymer film with liquid paraffin and the temperature kept constant under flowing N₂ gas. All of the structures were solved by a standard direct method (XSHELL V6.3.1 crystallographic software package of the Bruker AXS) and expanded Fourier techniques. Full-matrix least-squares refinements were carried out with anisotropic thermal parameters for all non-disordered and non-hydrogen atoms. All of the hydrogen atoms were placed in the measured positions and refined using a riding model. Relevant crystal data collection and refinement data for the crystal structures of 1 and 2 are summarized in Table S1. CCDC 2009750-2009752

Preparations

All chemicals were purchased from commercial sources and used without further purification. Precursor complex, $(\text{PPh}_4)_2[\text{ReN}(\text{CN})_4(\text{MeOH})]\cdot 3\text{MeOH}$ was prepared according to literature procedures.⁶ Compound $(\text{PPh}_4)_2[\text{Re}^{\text{V}}\text{N}(\text{CN})_4(\text{cypy})]\cdot 3\text{H}_2\text{O}$ (**1**), $(\text{PPh}_4)_2[\text{ReN}(\text{CN})_4(\text{MeOH})]\cdot 2\text{MeOH}\cdot 2\text{H}_2\text{O}$ (**2**) and $(\text{PPh}_4)_2[\text{Re}^{\text{V}}\text{N}(\text{CN})_4(\text{cypy})]\cdot 2\text{H}_2\text{O}$ (**1_EtOH**) were prepared by following steps.

Single Crystals of $(\text{PPh}_4)_2[\text{Re}^{\text{V}}\text{N}(\text{CN})_4(\text{cypy})]\cdot 3\text{H}_2\text{O}$ (**1**)

1 was prepared by a liquid phase diffusion method in a vial. $(\text{PPh}_4)_2[\text{ReN}(\text{CN})_4(\text{MeOH})]\cdot 3\text{MeOH}$ (50 mg, 0.05 mmol) was left at 95 °C for 4 hours in vacuo. The powder and 4-phenylpyridine (cypy) (234 mg, 2.25 mmol) were dissolved in acetone (15 mL) and then filtered to remove the remaining solid. Subsequently, 20 mL of diethylether was layered on the solution in a vial. The solution was allowed to stand for several days and the orange crystals formed were filtered. The crystals were dried in vacuo overnight and placed in the air for several days to give single crystals of **1**, exchanging crystal solvent acetone with water. Yield: 23.5 mg (41.2 %).

Anal. Calcd for $(\text{PPh}_4)_2[\text{Re}^{\text{V}}\text{N}(\text{CN})_4(\text{cypy})]\cdot 3\text{H}_2\text{O}$, $[\text{C}_{58}\text{H}_{50}\text{N}_7\text{O}_3\text{P}_2\text{Re}]$: C, 61.04; H, 4.42; N, 8.59. Found: C, 61.11; H, 4.39; N, 8.55. IR (cm^{-1}) 2125 ($\nu_{\text{C}\equiv\text{N}}$), 2103 ($\nu_{\text{C}\equiv\text{N}}$), 2094 ($\nu_{\text{C}\equiv\text{N}}$), 1604 ($\nu_{\text{ring}(\text{cypy})}$), 1546 ($\nu_{\text{ring}(\text{cypy})}$), 1416 ($\nu_{\text{ring}(\text{cypy})}$), 1079 ($\delta_{\text{ring}(\text{cypy})}$), 1066 ($\delta_{\text{ring}(\text{cypy})}$), 841 ($\gamma_{\text{ring}(\text{cypy})}$), 826 ($\gamma_{\text{ring}(\text{cypy})}$).

Single Crystals of $(\text{PPh}_4)_2[\text{ReN}(\text{CN})_4(\text{MeOH})]\cdot 2\text{MeOH}\cdot 2\text{H}_2\text{O}$ (**2**)

1 was placed under MeOH vapor for 3 hours to result in **2**, in which cypy was exchanged with MeOH.

Anal. Calcd for $(\text{PPh}_4)_2[\text{Re}^{\text{V}}\text{N}(\text{CN})_4(\text{MeOH})]\cdot 2\text{MeOH}\cdot 2\text{H}_2\text{O}$, $[\text{C}_{55}\text{H}_{55}\text{N}_5\text{O}_5\text{P}_2\text{Re}]$: C, 59.29; H, 4.98; N, 6.29. Found: C, 59.18; H, 4.94; N, 6.40. IR (cm^{-1}) 2135 ($\nu_{\text{C}\equiv\text{N}}$), 2117 ($\nu_{\text{C}\equiv\text{N}}$), 2104 ($\nu_{\text{C}\equiv\text{N}}$), 1084 ($\delta_{\text{H-O-C}(\text{MeOH})}$), 1036 ($\nu_{\text{C-O}(\text{MeOH})}$).

Single Crystals of $(\text{PPh}_4)_2[\text{ReN}(\text{CN})_4(\text{cypy})]\cdot 2\text{EtOH}$ (**1_EtOH**)

1 was placed under EtOH vapor for 3 hours to result in single crystals of **1_EtOH**.

Anal. Calcd for $(\text{PPh}_4)_2[\text{Re}^{\text{V}}\text{N}(\text{CN})_4(\text{cypy})]\cdot 2\text{EtOH}$, $[\text{C}_{62}\text{H}_{56}\text{N}_7\text{O}_2\text{P}_2\text{Re}]$: C, 63.14; H, 4.79; N, 8.31. Found: C, 63.43; H, 4.59; N, 8.28. IR (cm^{-1}) 2126 ($\nu_{\text{C}\equiv\text{N}}$), 2101 ($\nu_{\text{C}\equiv\text{N}}$), 1603 ($\nu_{\text{ring}(\text{cypy})}$), 1550 ($\nu_{\text{ring}(\text{cypy})}$), 1418 ($\nu_{\text{ring}(\text{cypy})}$), 1078 ($\delta_{\text{ring}(\text{cypy})}$), 1068 ($\delta_{\text{ring}(\text{cypy})}$), 830 ($\gamma_{\text{ring}(\text{cypy})}$).

Table S1. Crystallographic data and refinement parameter for **1**, **2**, and **1_EtOH**

	1 CCDC 2009750	2 CCDC 2009752	1_EtOH CCDC 2009751
Formula	C ₅₈ H ₅₀ N ₇ O ₃ P ₂ Re	C ₅₅ H ₄₃ N ₅ O ₅ P ₂ Re	C ₆₂ H ₅₆ N ₇ O ₂ P ₂ Re
Temperature / K	100	100	100
Crystal system	Triclinic	Triclinic	Triclinic
Space group	<i>P</i> $\bar{1}$	<i>P</i> $\bar{1}$	<i>P</i> $\bar{1}$
<i>a</i> / Å	13.556(3)	13.437(2)	13.6167(10)
<i>b</i> / Å	13.655(3)	13.848(3)	14.0119(10)
<i>c</i> / Å	16.754(3)	16.639(3)	15.9593(11)
α / °	71.320(2)	71.036(2)	109.2230(10)
β / °	88.136(2)	89.469(2)	90.4280(10)
γ / °	61.543(2)	61.390(2)	106.9900(10)
<i>V</i> / Å ³	2555.9(8)	2530.4(7)	2731.5(3)
<i>Z</i>	2	2	2
<i>GOF</i>	1.043	1.109	1.051
<i>R</i> ₁	2.44	3.86	2.47
<i>wR</i> ₂	5.18	8.56	5.95

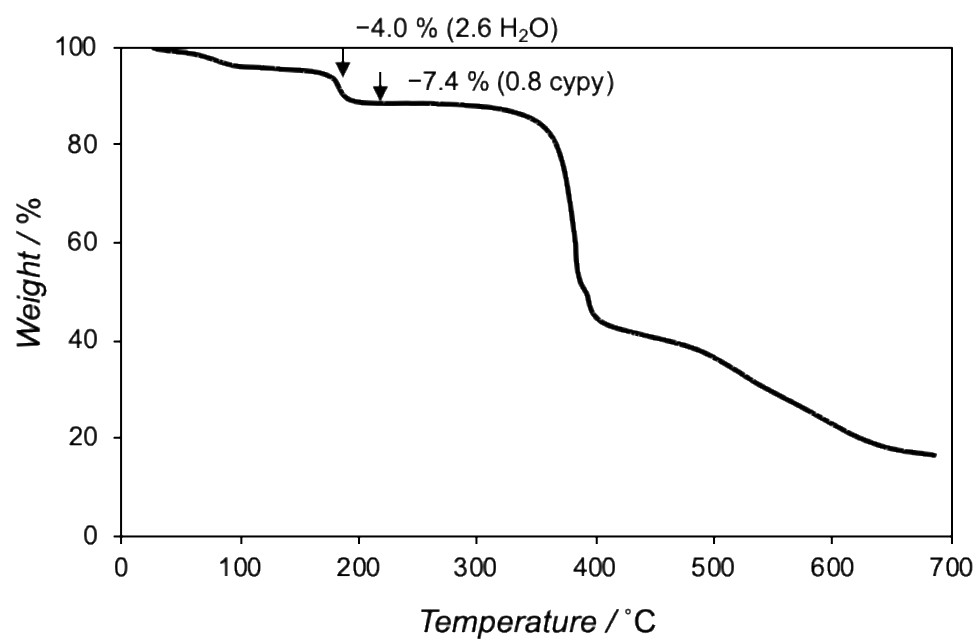


Fig. S1 Thermogravimetric analysis curves of **1**. Heating rate is 5 °C/min under N₂ flow.

Table S2. Selected bond distances and angles for **1**

Bond distances / Å			
Re(1)–N(1)	1.654(2)	C(1)–N(2)	1.152(3)
Re(1)–C(1)	2.108(3)	C(2)–N(3)	1.153(3)
Re(1)–C(2)	2.111(3)	C(3)–N(4)	1.160(3)
Re(1)–C(3)	2.105(3)	C(4)–N(5)	1.154(3)
Re(1)–C(4)	2.113(3)		
Re(1)–N(6)	2.569(2)		
Bond angles / °			
C(1)–Re(1)–C(2)	98.79(10)	Re(1)–C(1)–N(2)	178.9(2)
C(1)–Re(1)–C(3)	98.86(10)	Re(1)–C(2)–N(3)	179.8(3)
C(1)–Re(1)–C(4)	99.51(10)	Re(1)–C(3)–N(4)	178.0(2)
C(2)–Re(1)–C(3)	90.54(9)	Re(1)–C(4)–N(5)	176.1(2)
C(2)–Re(1)–C(4)	161.68(9)		
C(3)–Re(1)–C(4)	85.75(10)		
N(1)–Re(1)–N(6)	176.11(9)		

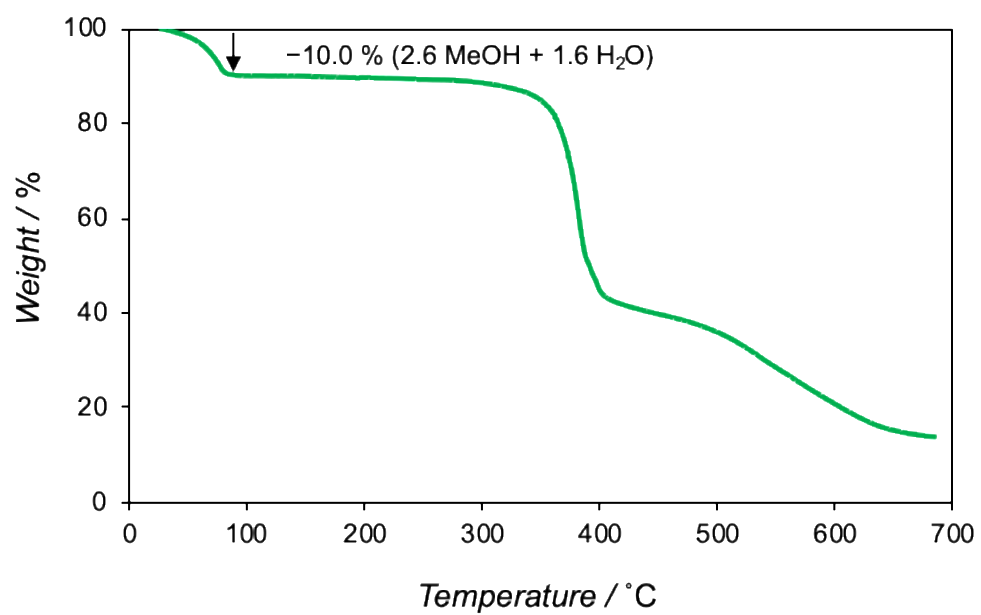


Fig. S2 Thermogravimetric analysis curves of **2**. Heating rate is 5 °C /min under N₂ flow.

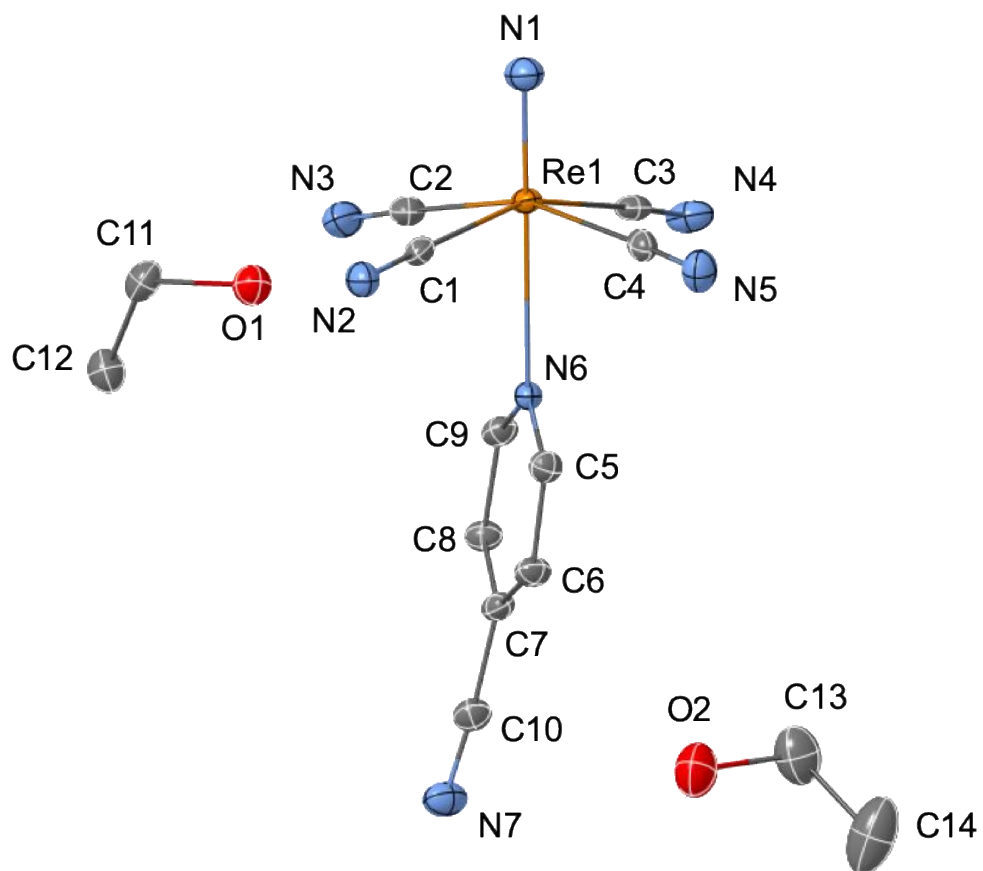


Fig. S3 Crystal structure of **1_EtOH**. PPh_4^+ cations and hydrogen atoms are omitted for clarity. Thermal ellipsoids are shown at the 50% probability level.

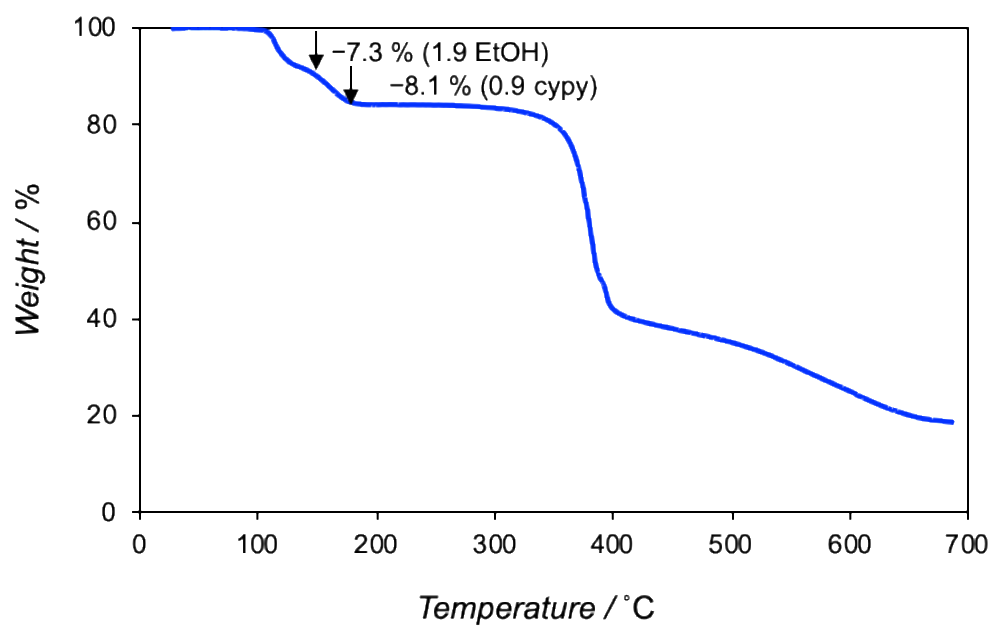


Fig. S4 Thermogravimetric analysis curves of **1_EtOH**. Heating rate is 5 °C/min under N₂ flow.

Table S3. Selected bond distances and angles for **2**

Bond distances / Å			
Re(1)–N(1)	1.667(4)	C(1)–N(2)	1.148(6)
Re(1)–C(1)	2.127(5)	C(2)–N(3)	1.150(6)
Re(1)–C(2)	2.105(5)	C(3)–N(4)	1.147(6)
Re(1)–C(3)	2.123(5)	C(4)–N(5)	1.156(6)
Re(1)–C(4)	2.100(5)		
Re(1)–O(1)	2.447(3)		
Bond angles / °			
C(1)–Re(1)–C(2)	88.41(17)	Re(1)–C(1)–N(2)	177.3(4)
C(1)–Re(1)–C(3)	164.19(17)	Re(1)–C(2)–N(3)	178.1(5)
C(1)–Re(1)–C(4)	89.97(18)	Re(1)–C(3)–N(4)	176.0(4)
C(2)–Re(1)–C(3)	90.34(16)	Re(1)–C(4)–N(5)	177.8(4)
C(2)–Re(1)–C(4)	160.63(18)		
C(3)–Re(1)–C(4)	86.00(17)		
N(1)–Re(1)–O(1)	178.57(17)		

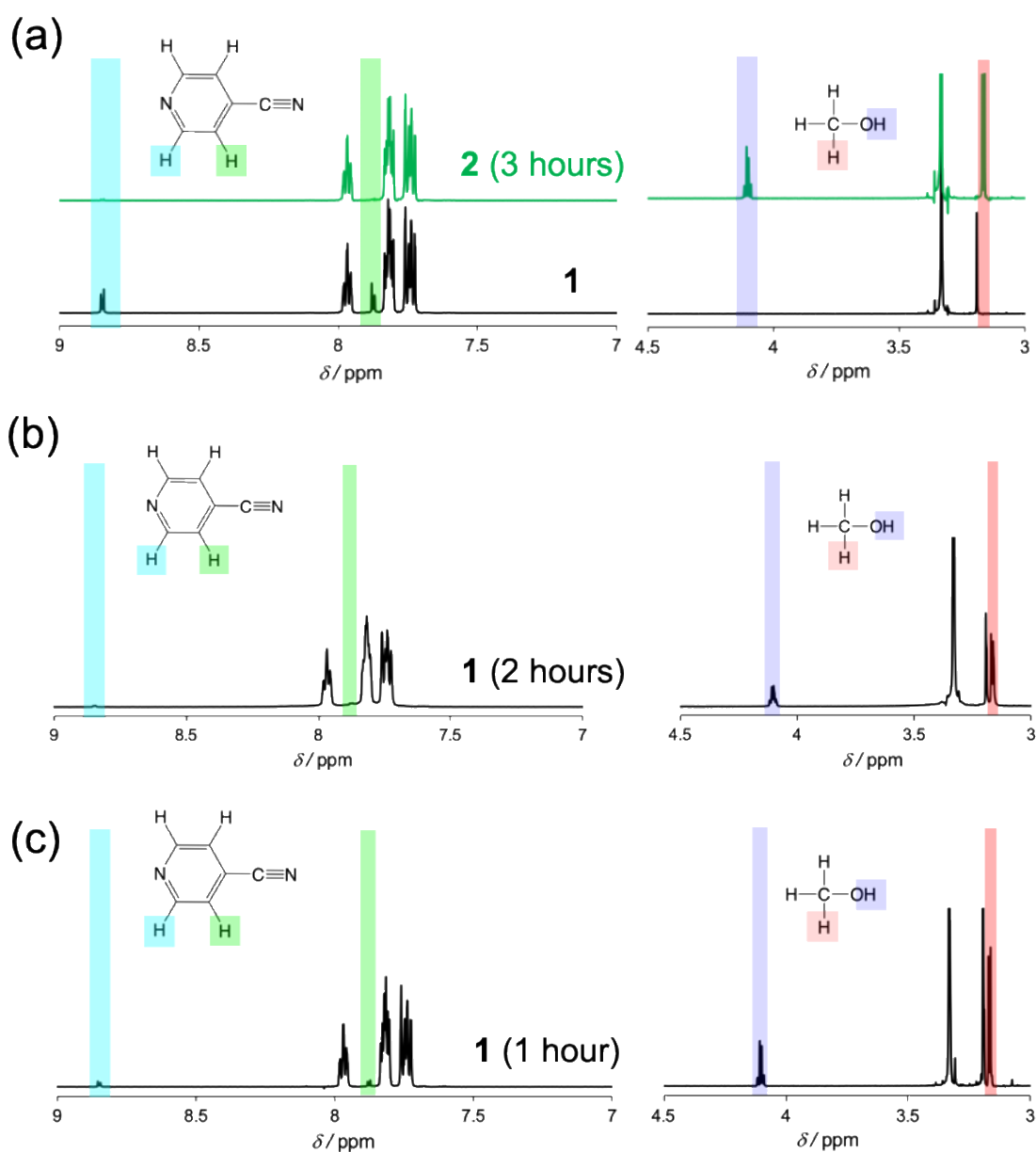


Fig. S5 (a) ¹H-NMR spectra for **1** and **2** in DMSO-*d*₆ at 600 MHz. **1**: δ (ppm) = 8.84 (2H; d, pyridyl proton of cypy), 7.97 (8H; t, phenyl proton of PPh₄⁺ cations), 7.87 (2H; d, pyridyl proton of cypy), 7.81 (16H; t, phenyl proton of PPh₄⁺ cations), 7.74 (8H; d, phenyl proton of PPh₄⁺ cations), and 7.73 (8H; d, phenyl proton of PPh₄⁺ cations). The humps around 3.33 ppm is due to the protonated water (HOH) and the humps around 3.19 ppm is due to the protonated water (HOD).

2: δ = 7.97 (8H; t, phenyl proton of PPh_4^+ cations), 7.81 (16H; t, phenyl proton of PPh_4^+ cations), 7.75 (8H; d, phenyl proton of PPh_4^+ cations), and 7.73 (8H; d, phenyl proton of PPh_4^+ cations), 4.10 (1H; q, hydroxy proton of MeOH) and 3.17 (3H; d, methyl proton of MeOH). The humps around 3.33 ppm is due to the protonated water (HOH) and the humps around 3.19 ppm is due to the protonated water (HOD).

(b) ^1H -NMR spectra for MeOH diffused **1** for two hours in $\text{DMSO-}d_6$ at 600 MHz. δ (ppm) = 8.83 (2H; d, pyridyl proton of cypy), 7.97 (8H; t, phenyl proton of PPh_4^+ cations), 7.86 (2H; d, pyridyl proton of cypy), 7.82 (16H; t, phenyl proton of PPh_4^+ cations), 7.75 (8H; d, phenyl proton of PPh_4^+ cations), and 7.73 (8H; d, phenyl proton of PPh_4^+ cations), 4.10 (1H; q, hydroxy proton of MeOH) and 3.17 (3H; d, methyl proton of MeOH). The humps around 3.33 ppm is due to the protonated water (HOH) and the humps around 3.19 ppm is due to the protonated water (HOD).

(c) ^1H -NMR spectra for MeOH diffused **1** for one hour in $\text{DMSO-}d_6$ at 600 MHz. δ (ppm) = 8.84 (2H; d, pyridyl proton of cypy), 7.97 (8H; t, phenyl proton of PPh_4^+ cations), 7.87 (2H; d, pyridyl proton of cypy), 7.82 (16H; t, phenyl proton of PPh_4^+ cations), 7.75 (8H; d, phenyl proton of PPh_4^+ cations), and 7.74 (8H; d, phenyl proton of PPh_4^+ cations), 4.10 (1H; q, hydroxy proton of MeOH) and 3.17 (3H; d, methyl proton of MeOH). The humps around 3.33 ppm is due to the protonated water (HOH) and the humps around 3.19 ppm is due to the protonated water (HOD).

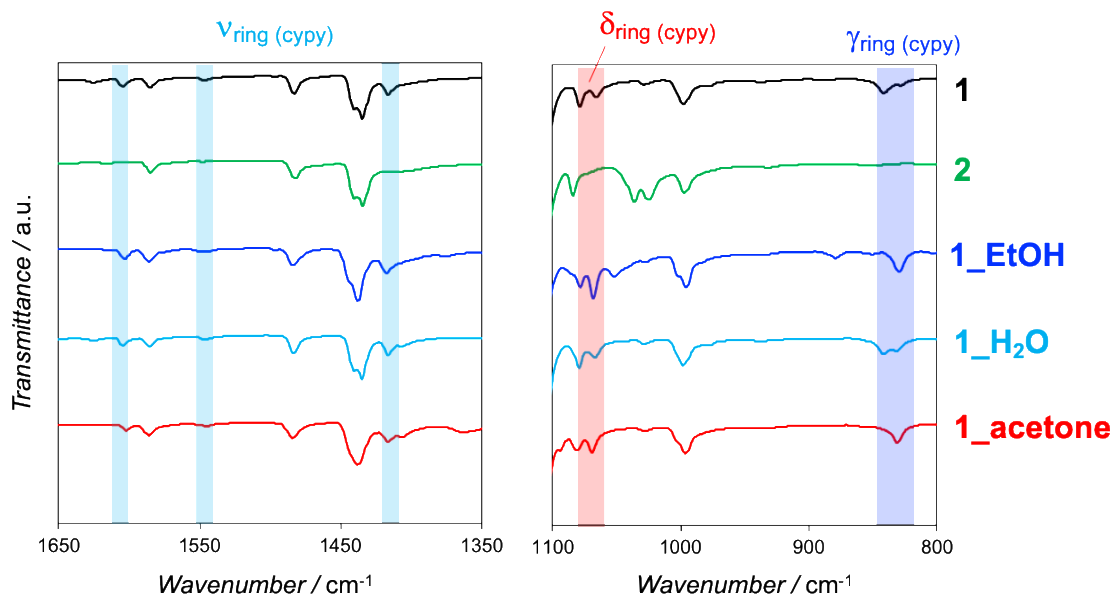


Fig. S6 FT-IR spectra of **1** (black), **1_{guest}** (MeOH (**2**): green, EtOH: blue, H₂O: light blue, acetone: red).

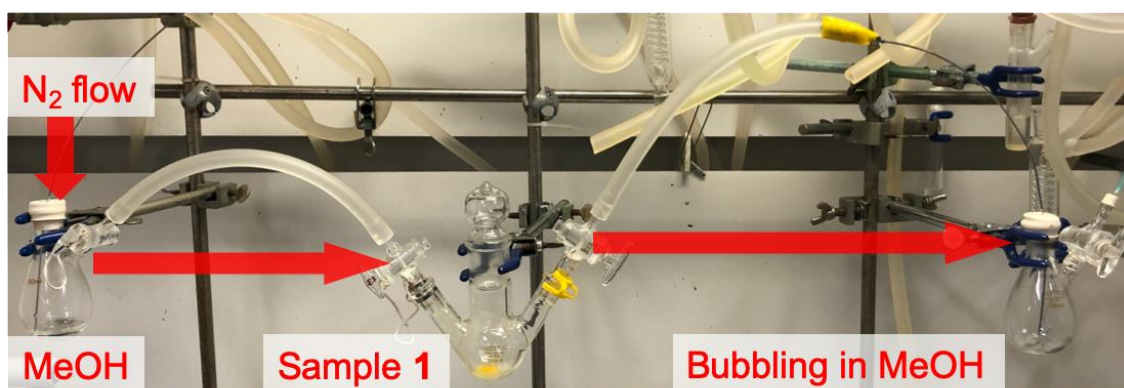


Fig. S7 Experimental equipment for UV-vis adsorption measurement. N_2 gas was bubbled in MeOH (left vessel) and then MeOH vapor flowed into sample **1** (middle vessel). Subsequently, the vapor which went through **1** was bubbled in MeOH (right vessel). The final MeOH solution was undergone UV-vis adsorption measurement.

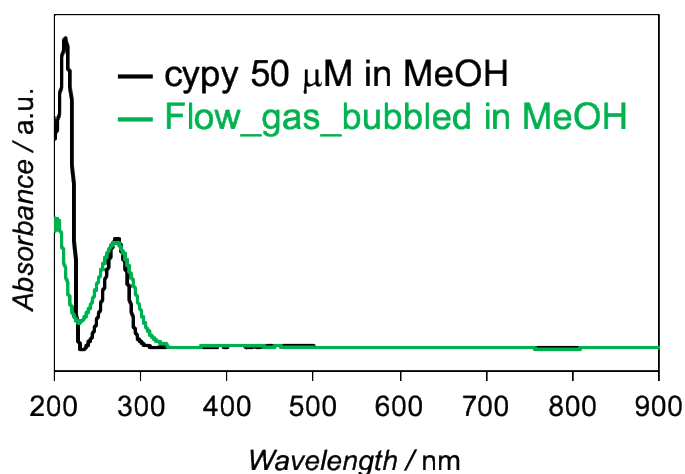


Fig. S8 UV-vis adsorption spectra of above-mentioned flow gas bubbled MeOH solution (green) and 50 μM cypy methanolic solution (black). Baseline is taken with N_2 bubbled MeOH. The adsorption peaks around 205 nm and 270 nm were in good agreement with those of spectrum of 50 μM cypy in methanolic solution

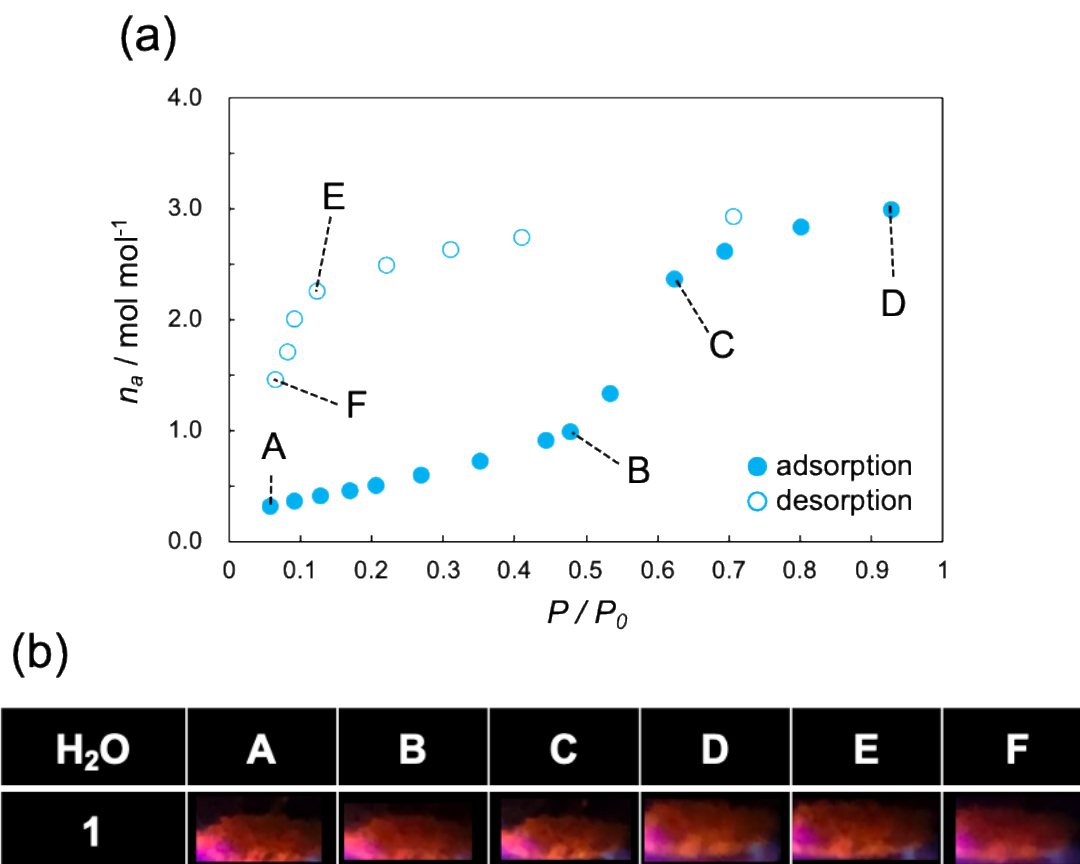
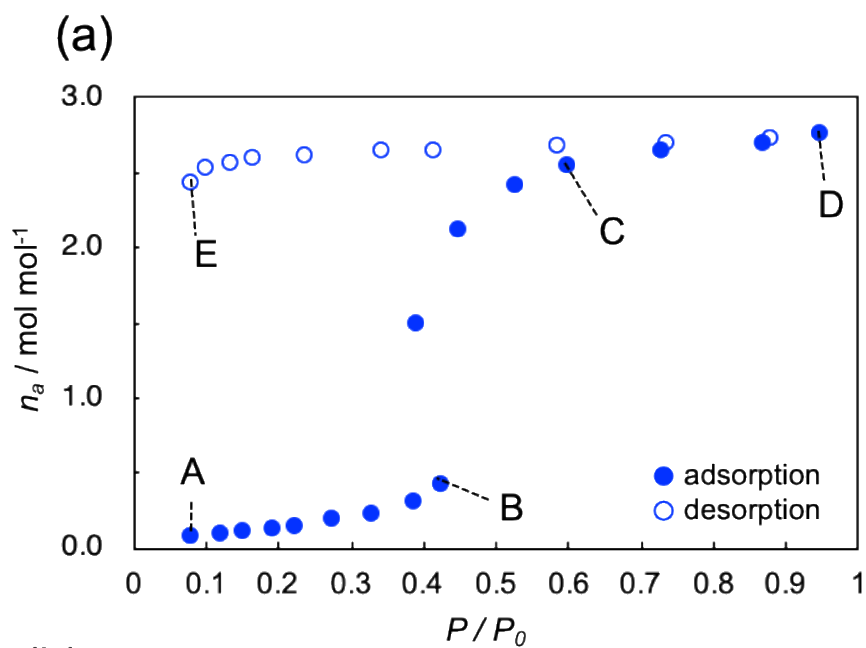


Fig. S9 (a) H₂O adsorption isotherms of **1_dehyd** at 298K and (b) photos under UV light at each relative pressure. They were taken at A: $P/P_0 = 0.06$, B: $P/P_0 = 0.48$, C: $P/P_0 = 0.70$, D: $P/P_0 = 0.93$ in adsorption curve and E: $P/P_0 = 0.12$, F: $P/P_0 = 0.07$ in desorption curve.



(b)

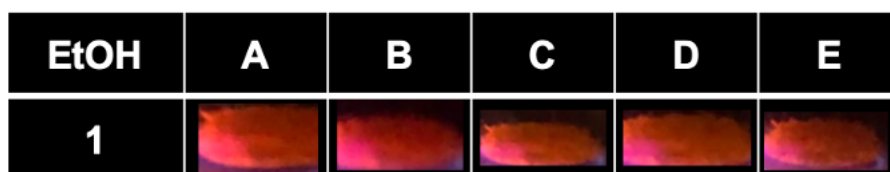


Fig. S10 (a) EtOH adsorption isotherms of **1_dehyd** at 298K and (b) photos under UV light at each relative pressure. They were taken at A: $P/P_0 = 0.08$, B: $P/P_0 = 0.43$, C: $P/P_0 = 0.60$, D: $P/P_0 = 0.95$ in adsorption curve and E: $P/P_0 = 0.10$ in desorption curve.

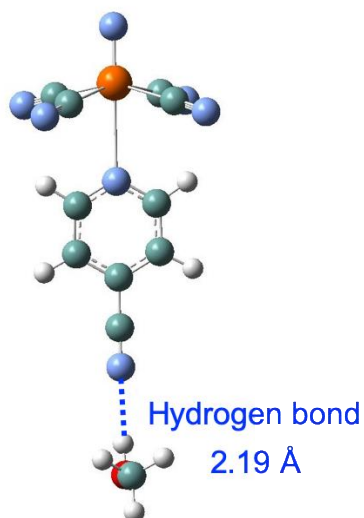


Fig. S11 Optimized geometries of **1** and MeOH molecule in the ground state calculated at the SDD/6-311G (+d) basis set. $[\text{Re}^{\text{V}}\text{N}(\text{CN})_4(\text{cypy})]^{2-}$ unit was modeled using crystal information file (cif) and MeOH was arbitrarily placed beneath cypy. Hydrogen bond distance between $\text{N}(\text{cypy})\cdots\text{H}(\text{MeOH})$ is 2.19 Å and $\text{Re}\cdots\text{N}(\text{cypy})$ distance was extended to 2.82 Å (original length is 2.56 Å). It is needless to say acetone molecules were not able to form hydrogen bond due to lack of hydrogen atoms. That is why acetone did not induce the ligand exchange reaction.

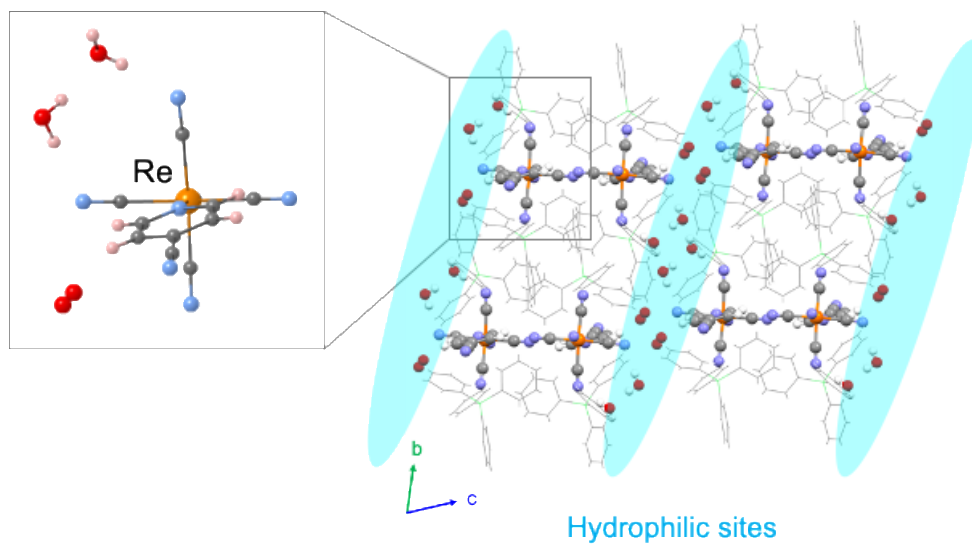


Fig. S12 Packing structure of **1**. H₂O crystal solvents were found in relatively hydrophilic sites which is far from PPh₄⁺ cations. PPh₄⁺ cations are modeled by wireframe style for clarity.

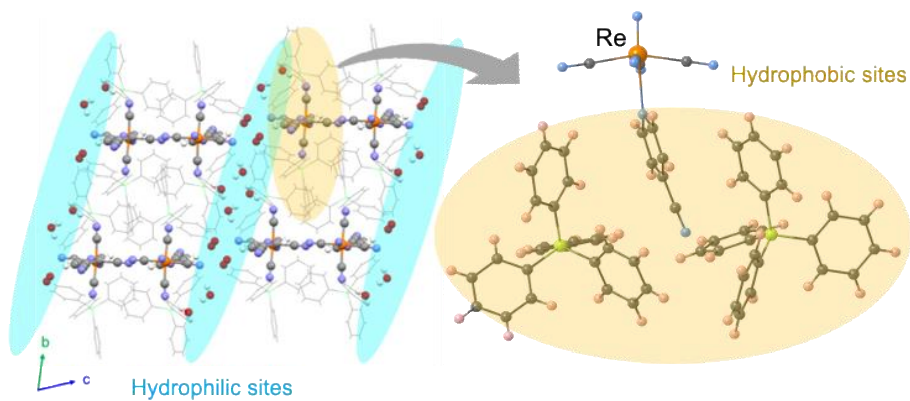


Fig. S13 Packing structure of **1** and hydrophobic sites around cyp.

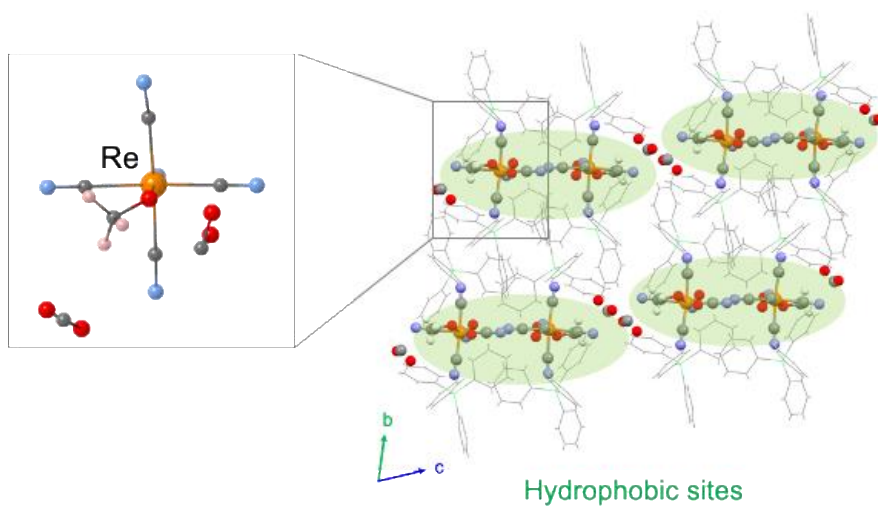


Fig. S14 Packing structure of **2**. MeOH crystal solvents were found in both hydrophilic and hydrophobic sites. PPh_4^+ cations are modeled by wireframe style for clarity. H_2O molecules are omitted for clarity.

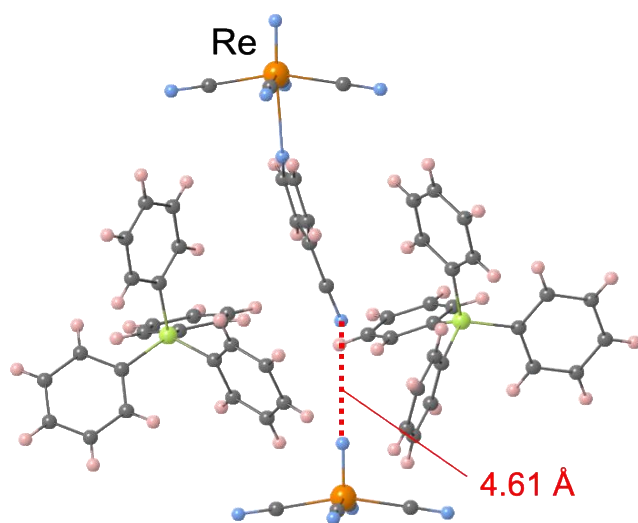
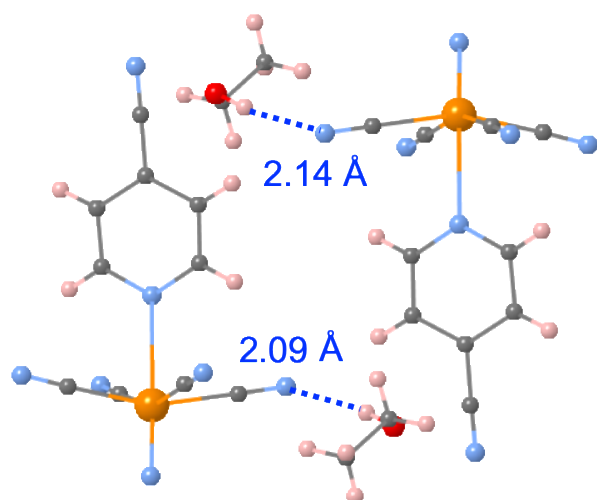


Fig. S15 Packing structure of **1**. cpy and nitride distance is about 4.61 Å.



Hydrogen Bond

Fig. S16 Packing structure of **1_EtOH**. EtOH was found only as crystal solvents and they form hydrogen bonds with cyano groups of $[\text{Re}^{\text{V}}\text{N}(\text{CN})_4(\text{cypy})]^{2-}$. PPh_4^+ cations are omitted for clarity.

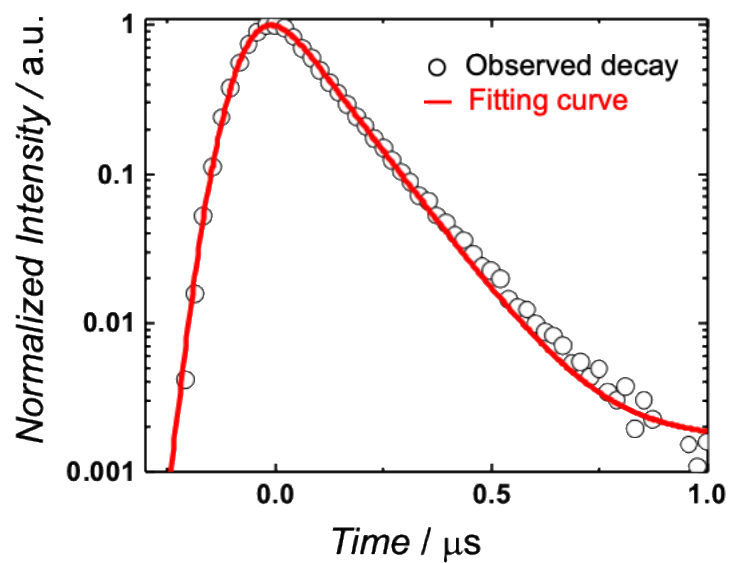


Fig. S17 Time-resolved PL decay ($\lambda_{\text{ex}} = 355 \text{ nm}$) at room temperature of **1**.

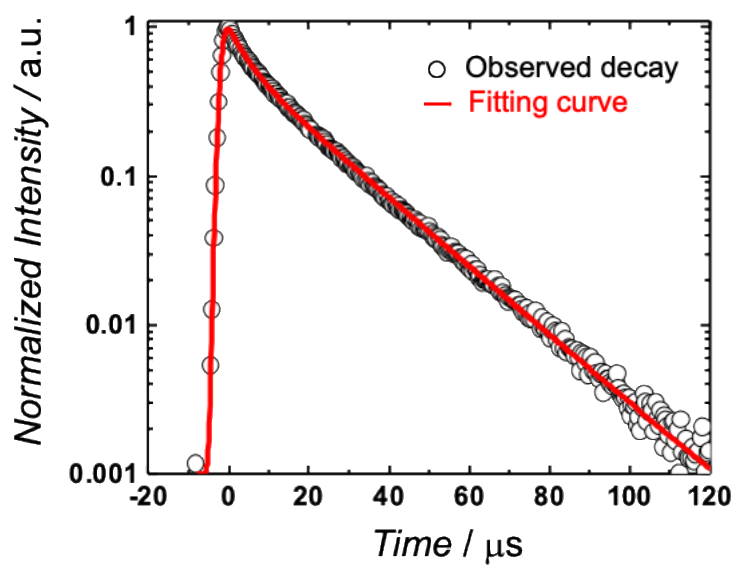


Fig. S18 Time-resolved PL decay ($\lambda_{\text{ex}} = 355 \text{ nm}$) at room temperature of **2**.

Reference

- 1 (a) W. R. Dawson and M. W. Windsor, *J. Phys. Chem.*, 1968, **72**, 3251-3260
(b) W. H. Melhuish, *J. Phys. Chem.*, 1961, **65**, 229-235.
- 2 R. D. Spencer and G. Weber, *J. Chem. Phys.*, 1970, **52**, 1654-1663.
- 3 GaussView, Version 6.1, Roy Dennington, Todd A. Keith, and John M. Millam, Semichem Inc., Shawnee Mission, KS, 2016.
- 4 Gaussian 16, Revision C.01, M. J. Frisch, G. W. Trucks, H. B. Schlegel, G. E. Scuseria, M. A. Robb, J. R. Cheeseman, G. Scalmani, V. Barone, G. A. Petersson, H. Nakatsuji, X. Li, M. Caricato, A. V. Marenich, J. Bloino, B. G. Janesko, R. Gomperts, B. Mennucci, H. P. Hratchian, J. V. Ortiz, A. F. Izmaylov, J. L. Sonnenberg, D. Williams-Young, F. Ding, F. Lipparini, F. Egidi, J. Goings, B. Peng, A. Petrone, T. Henderson, D. Ranasinghe, V. G. Zakrzewski, J. Gao, N. Rega, G. Zheng, W. Liang, M. Hada, M. Ehara, K. Toyota, R. Fukuda, J. Hasegawa, M. Ishida, T. Nakajima, Y. Honda, O. Kitao, H. Nakai, T. Vreven, K. Throssell, J. A. Montgomery, Jr., J. E. Peralta, F. Ogliaro, M. J. Bearpark, J. J. Heyd, E. N. Brothers, K. N. Kudin, V. N. Staroverov, T. A. Keith, R. Kobayashi, J. Normand, K. Raghavachari, A. P. Rendell, J. C. Burant, S. S. Iyengar, J. Tomasi, M. Cossi, J. M. Millam, M. Klene, C. Adamo, R. Cammi, J. W. Ochterski, R. L. Martin, K. Morokuma, O. Farkas, J. B. Foresman, and D. J. Fox, Gaussian, Inc., Wallingford CT, 2016.
- 5 O. V. Dolomanov, L. J. Bourhis, R. J. Gildea, J. a. K. Howard and H. Puschmann, *J. Appl. Crystallogr.*, 2009, **42**, 339-341.
- 6 H. Ikeda, T. Yoshimura, A. Ito, E. Sakuda, N. Kitamura, T. Takayama, T. Sekine and A. Shinohara, *Inorg. Chem.*, 2012, **51**, 12065-12074.